Supplemental Information, Fig.S7

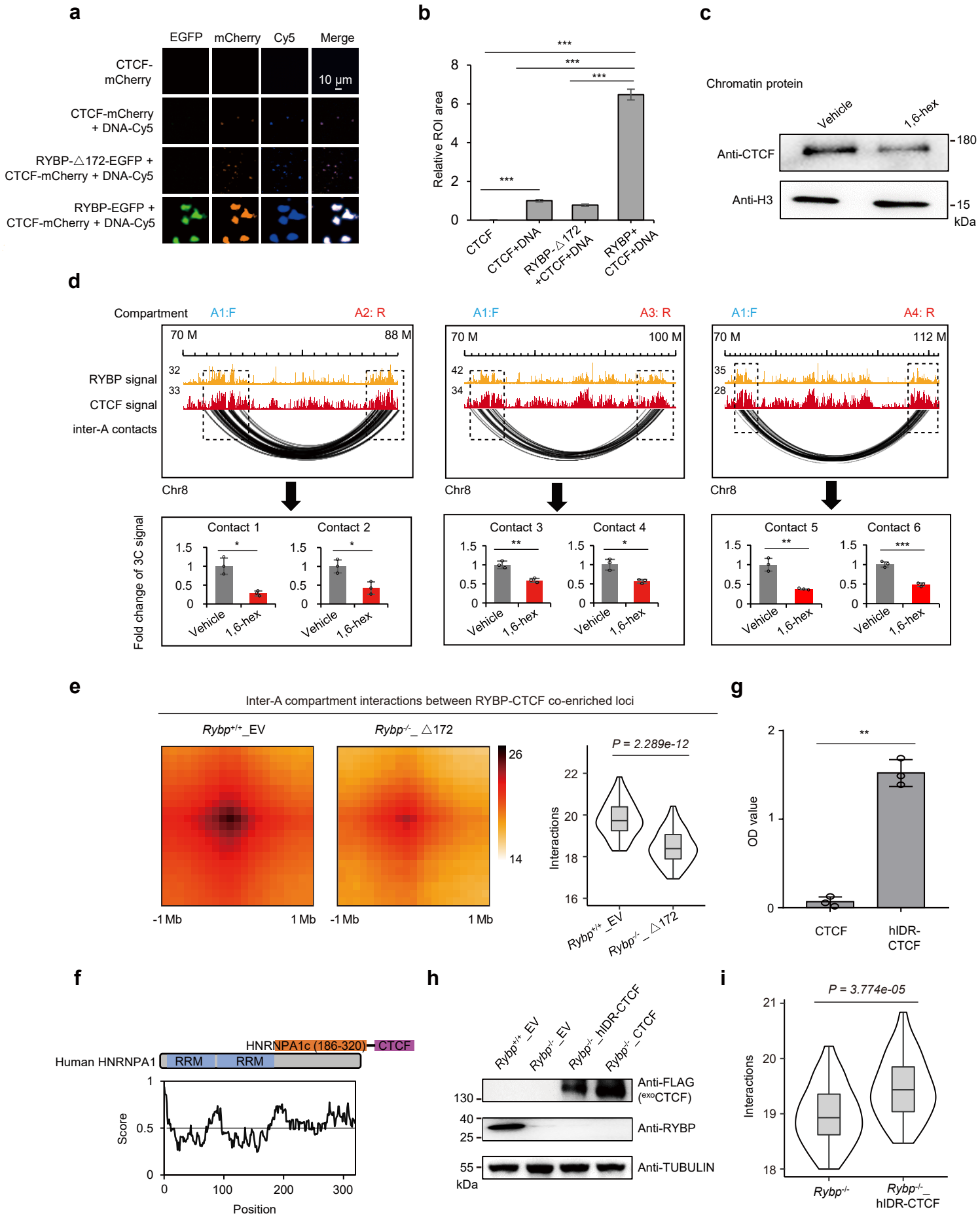

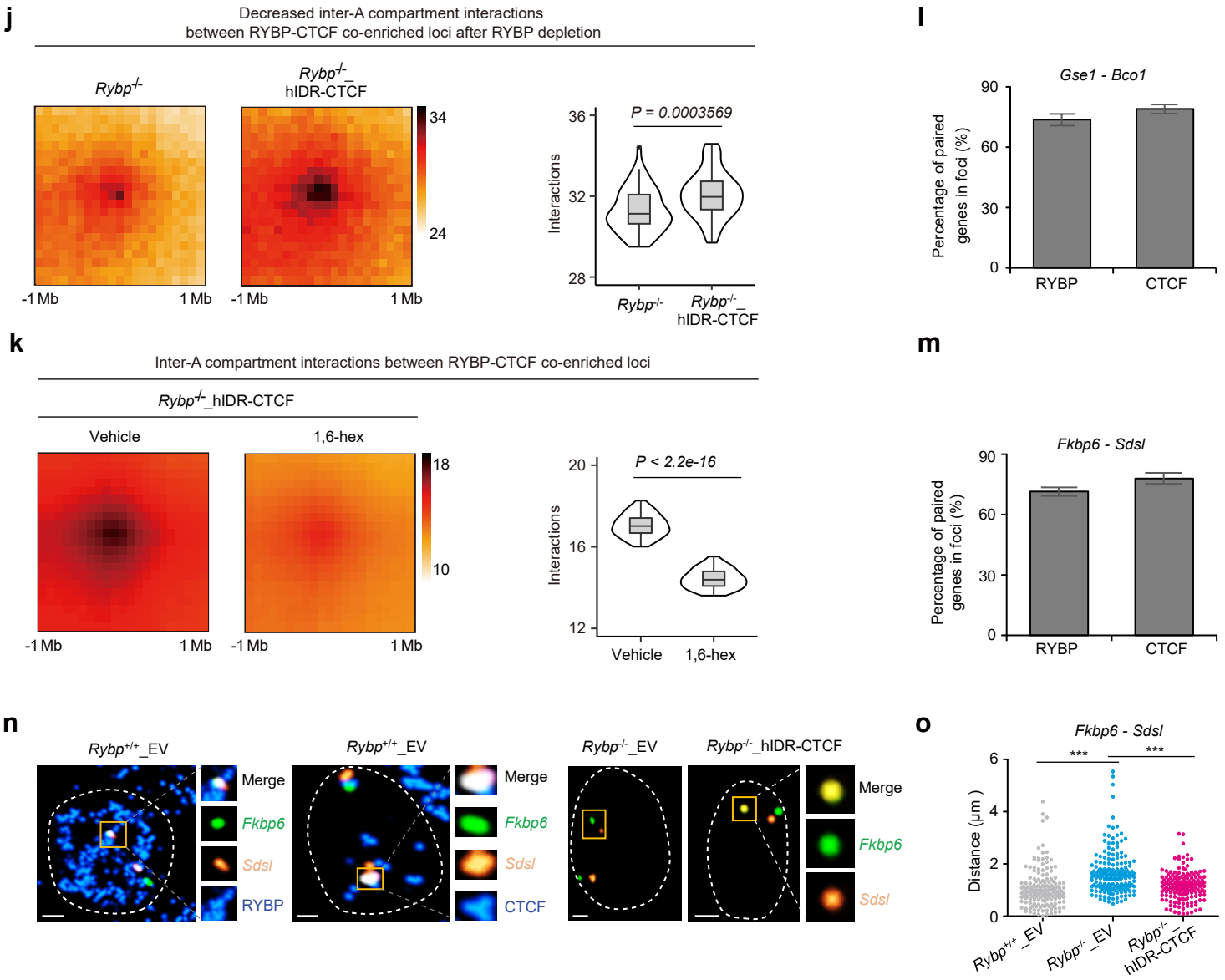
j
Decreased inter-A compartment interactions
between RYBP-CTCF co-enriched loci after RYBP depletion
Rybp-/-
Rybp-/-_
hIDR-CTCF
34
24
-1 Mb
1 Mb
-1 Mb
1 Mb
P = 0.0003569
36
32
28
Interactions
Rybp-/-
Rybp-/-_
hIDR-CTCF
l
Gse1 - Bco1
90
60
30
0
Percentage of paired
genes in foci (%)
RYBP
CTCF
k
Inter-A compartment interactions between RYBP-CTCF co-enriched loci
Rybp-/-_hIDR-CTCF
Vehicle
1,6-hex
18
10
-1 Mb
1 Mb
-1 Mb
1 Mb
P < 2.2e-16
20
16
12
Interactions
Vehicle
1,6-hex
m
Fkbp6 - Sdsl
90
60
30
0
Percentage of paired
genes in foci (%)
RYBP
CTCF
n
Rybp+/+_EV
Rybp+/+_EV
Rybp-/-_EV
Rybp-/-_hIDR-CTCF
Merge
Fkbp6
Sdsl
RYBP
Merge
Fkbp6
Sdsl
CTCF
Merge
Fkbp6
Sdsl
o
Fkbp6 - Sdsl
***
***
6
4
2
0
Distance (µm)
Rybp+/+_EV
Rybp-/-_EV
Rybp-/-_
hIDR-CTCF

Supplementary information, Fig.S7 Induced CTCF phase separation restores inter-A compartment interactions impaired by RYBP depletion. a, b In the presence of PEG8000, representative images (**a**) and statics (**b**) of CTCF-mCherry aggregation after addition of Cy5-labbled 25×DNA motif, RYBP-△172-EGFP or full-length RYBP-EGFP. The concentration of RYBP-EGFP and RYBP-△172-EGFP were 40 μM, CTCF-mCherry was 0.8 μM. Welch's *t*-test; n values are (from left to right): n = 0; n = 187; n = 127; n = 196. All the P values are (from left to right): $P < 2.2e\text{-}16$. **c** Western blot showing the reduced binding of CTCF at chromatin after 1,6-hex treatment. **d** Top: The zoom-in browser view of interactions between two A compartments from CTCF ChIA-PET data (GSM2645441). Bottom: 3C-qPCR showing the decreased interactions between the two A compartments after 1,6-hex treatment. Welch's *t*-test; P values are (from left to right): $P = 0.0235$; $P = 0.0379$; $P = 0.0016$; $P = 0.01088$; $P = 0.0016$; $P = 0.0002$, n =3. **e** APA plots (left) and quantitation (right) showing the genome-wide aggregate strength between RYBP-CTCF co-enriched loci from different A compartments after RYBP mutation, Wilcoxon rank-sum test. **f** Human HNRNPA1 (left) is intrinsically disordered protein predicted by IUPred2A. The C-term IDR (186-320, yellow frame) of HNRNPA1 was fused with full-length CTCF. The human HNRNPA1 shows low homology with mouse HNRNPA1. **g** Turbidity assay showing the droplet formation of WT or hIDR-CTCF without PEG8000, 10 μM WT or hIDR-CTCF were used. Welch's *t*-test; all n values are 3; P = 0.001446. **h** Western blot showing the expression of exogenous hIDR-CTCF and exogenous CTCF (^{exo}CTCF) in ESCs. **i** Quantitation of APA showing the genome-wide aggregate strength between RYBP-CTCF co-enriched loci from different A compartments after inducing CTCF phase separation, Wilcoxon rank-sum test. **j** APA plots (left) and quantitation (right) showing the genome-wide aggregate strength between RYBP-CTCF co-enriched loci after inducing CTCF phase separation, the most strongly decreased (top 10%) inter-A compartment interactions between RYBP-CTCF co-enriched loci after RYBP depletion were

used for the analysis, Wilcoxon rank-sum test. **k** APA plots (left) and quantitation (right) showing the genome-wide aggregate strength between RYBP-CTCF co-enriched loci from different A compartments after 1,6-hex treatment in *Rybp*$^{-/-}$_hIDR-CTCF mESCs, Wilcoxon rank-sum test. **l, m** The percentage of interacted genes in RYBP or CTCF puncta. **n** DNA FISH coupled with RYBP or CTCF immunofluorescence displaying the *Fkbp6* (green) and *Sdsl* (yellow) are interacted in RYBP or CTCF puncta, and distance change in *Rybp*$^{-/-}$_EV mESCs and *Rybp*$^{-/-}$_hIDR-CTCF mESCs, the two genes localized in RYBP-CTCF co-enriched loci, all the scale bars denote 2 μm. **o** The distance change between *Fkbp6* and *Sdsl* in different cell lines. Welch's *t*-test; *Rybp*$^{+/+}$_EV: n = 181; *Rybp*$^{-/-}$_EV: n = 182; *Rybp*$^{-/-}$_hIDR-CTCF: n = 167; P values are (from left to right): *P* = 1.0549e-10; *P* = 2.112e-10.